Probabilistic Oblique Impact Analysis of Functionally Graded Plates – A Multivariate Adaptive Regression Splines Approach

P. K. Karsh[1,*], Bindi Thakkar[1], R. R. Kumar[2,*], Vaishali[3] and Sudip Dey[3]

[1]*Department of Mechanical Engineering, Parul Institute of Engineering & Technology, Parul University, Vadodara, India*
[2]*Department of Aeronautical Engineering; Hindustan Institute of Technology and Science, Chennai, India*
[3]*Department of Mechanical Engineering, National Institute of Technology Silchar, India*
E-mail: pradeepkarsh@gmail.com; ravirk@hindustanuniv.ac.in
[*]*Corresponding Author*

Received 29 May 2021; Accepted 27 August 2021;
Publication 06 October 2021

Abstract

Purpose: To investigate the probabilistic low-velocity impact of functionally graded (FG) plate using the MARS model, considering uncertain system parameters.

Design/methodology/application: The distribution of various material properties throughout FG plate thickness is calculated using power law. For finite element (FE) formulation, isoparametric elements with eight nodes are considered, each component has five degrees of freedom. The combined effect of variability in material properties such as elastic modulus, modulus of rigidity, Poisson's ratio, and mass density are considered. The surrogate model is validated with the FE model represented by the scatter plot and

European Journal of Computational Mechanics, Vol. 30_2–3, 223–254.
doi: 10.13052/ejcm2642-2085.30234

the probability density function (PDF) plot based on Monte Carlo simulation (MCS).

Findings: The outcome of the degree of stochasticity, impact angle, impactor's velocity, impactor's mass density, and point of impact on the maximum value of contact force (CF_{max}), plate deformation (PD_{max}), and impactor deformation (ID_{max}) are determined. A convergence study is also performed to determine the optimal number of the constructed MARS model's sample size.

Originality/value: The results illustrate the significant effects of uncertain input parameters on FGM plates' low-velocity impact responses by employing a surrogate-based MARS model.

Keywords: Uncertainty, low-velocity impact, functionally graded materials (FGM), Monte Carlo simulation (MCS), multivariate adaptive regression splines (MARS).

Nomenclature

Symbols	***Descriptions***
$[M(\hat{\omega})]$	global mass matrix
$[K(\hat{\omega})]$	global stiffness matrix
$\{\delta\}$	global displacement vector
$\{F_C^*\}$	contact force
$m_{(I)}$	impactor's mass
$\ddot{\delta}_{(I)}$	acceleration
K_M	modified contact stiffness
ψ	local indentation
$\psi_{\max.}$	maximum indentation
C and λ	constants
δ_I	impactor deformation
δ_P	plate deformation
θ	impact angle
ϕ	twist angle
Δt	time interval
$[\tilde{K}_P]$	stiffness matrix for target plate
$[\tilde{K}_I]$	stiffness matrix for impactor
$\hat{S}_i$	shape function

ε and ϑ	local and natural coordinates
E_{Al}, E_{Zr}	elastic modulus of aluminium and zirconia
μ_{Al}, μ_{Zr}	Poisson's ratio of aluminium and zirconia
ρ_{Al}, ρ_{Zr}	mass density of aluminium and zirconia
p	power law index
t	plate thickness
$(\hat{\omega})$	degree of stochasticity
$f(x)$	Basic function
γ	constant coefficient
i_n	interaction order
$q_{i,n}$	knot position of corresponding variables
T	truncated power function
Φ	MCS operator
FGM	Functionally Graded Materials
MCS	Monte Carlo Simulations
MARS	Multivariate Adaptive Regression Splines
$\mathrm{CF}_{\max}$	maximum value of contact force
$\mathrm{PD}_{\max}$	maximum value of plate deformation
$\mathrm{ID}_{\max}$	maximum value of impactor deformation
MHC	modified Hertzian contact
N	sample size

1 Introduction

FGM are materials with composition and structural variation throughout their volume, with improved mechanical properties like high corrosion and heat resistance. They are an engineering approach to modify the structural or chemical arrangement of materials and elements. The term "functionally graded material "differs from composite materials. As well known, the composite material includes two or more components with different physical and chemical compositions. But FGM may be mono-componential material with gradient caused, for example, by non-uniform (gradient) distribution of residual stresses. The term FGM reflects the functional aspect of materials characterization; on the other hand, the name "composite material" relates to the structural organization. The mechanical and thermal properties of FGM are better than that of the laminated composites. As, in FGM there is no interlaminate joint, internal stresses, delamination, and improper bonding present. In addition, FGM has good thermal resistance provided by ceramic materials, while the metal component is responsible for high mechanical

strength. Due to these enhanced properties, it is used as a thermal barrier and lightweight structure. These materials also find applications in industries like aerospace, computer circuits are developing materials that can withstand very high thermal gradients. Also, in medical implants, graded materials are used for total replacements of the knee and hips. FGMs' advanced mechanical properties such as corrosion resistance, malleability, toughness, and fracture resistance help them to widen their application. Therefore, the present study is focused on FGM.

FGMs have most of the applications in aerospace, civil construction, marine industries. Therefore, they are mostly subjected to dynamic responses. Hence, it is essential to carry out its dynamic analysis for the reliability and safety of such structures. Many works have been carried out on these structures, such as vibration analysis of FGM by Darilmaz (2015), Belkorissat (2015), Atmane (2011). Considering buckling behaviour, some studies were conducted by Fekrar (2012), Chaht (2015), Tebboune (2015). Considering FGM's impact behavior, Singh et al. (2017) studied the effects of low-velocity impact responses using modified Hertzian contact law (MHCL) to characterize functionally graded material properties. Hou et al. (2019) worked on repaired CFRP laminates and analyzed the effects of loading position, while He et al. 2019) determined the influence of the aluminum honeycomb sandwich's structure parameters. Mars et al. (2018) investigate the impact behavior of glass fiber-reinforced polyamide by employing experimental and numerical methods. Shariyat and Jafari (2013a) performed a nonlinear impact analysis of an FGM plate subjected to radial load utilizing a novel refined contact stiffness approach. The gradation of material properties was carried out in both radial and transverse directions. Etemadi et al. (2009) and Apetre et al. (2006) carried out a three-dimensional FEN simulation for impact on a sandwich plate with an FGM core and found various outcomes on the impactor, such as velocity kinetic energy, beam dimensions on the indentation and displacements. Gong et al. (1999) applied the analytical method for analyzing the impact responses on FG shells with single and multiple layers. They evaluated the outcome of the volume fraction of constituents and configuration. Chelu and Librescu (2006) worked on FG circular plate to analyze its impact responses and used the Wavelet-Galerkin scheme, classical lamination plate theory, Hertzian contact law, and determined the contact force and penetration, displacement of the plate. Fu et al. (2016) worked on FG spherical shell. They conducted the numerical analysis for the nonlinear impact behavior in a thermal environment utilizing the Chebyshev collocation method and Newmark scheme. At the same time, Shariyat and Jafari (2013b) applied a

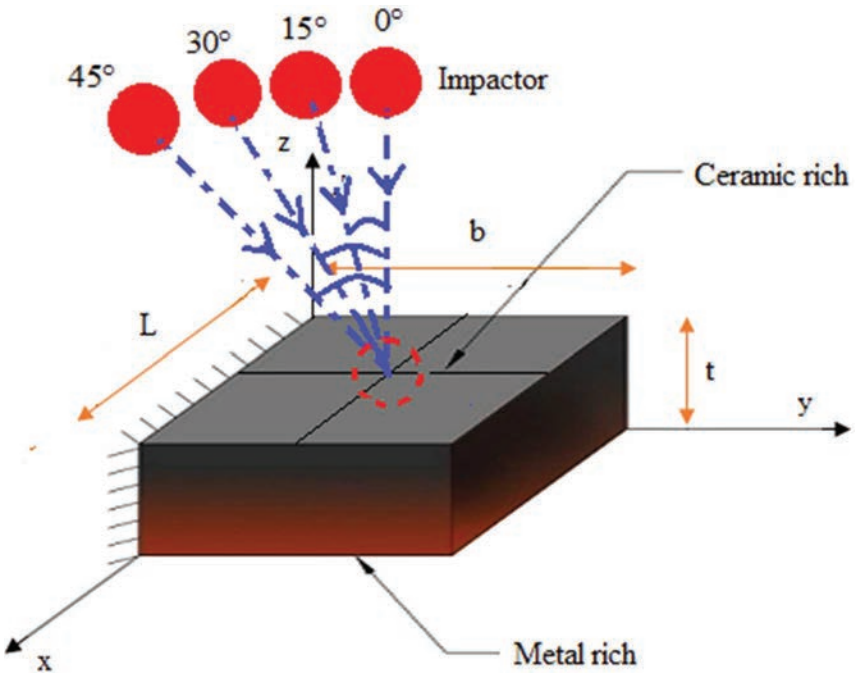

Figure 1 FGM cantilever plate subjected to impact loading.

micromechanical approach on two-dimensional FGM circular plates. From the discussion in the above paragraph, it can be concluded that mostly the work on FGM subjected to dynamic response is carried out considering a deterministic approach. In real-life situations, many kinds of uncertainties are present, which are unavoidable. So, for the safety and reliability of these structures, these uncertainties should also be considered during analysis. Some researchers worked on FGM considering uncertainties; such as Dey et al. (2015), Dey and Karmakar (2014a), Dey and Karmakar (2014b), Gao et al. (2018), Karsh et al. (2019), worked on FGM and composite structures considering stochastic impact responses. It is observed that limited literature is present considering stochastic impact response. Therefore, the present study focuses on the stochastic impact behavior of the FGM plate.

The most common method for performing stochastic analysis is the Monte Carlo simulation technique. However, this technique is quite a computationally exhaustive process. It requires a minimum of ten thousand simulations to predict the results, resulting in much time consumption accurately. Therefore, to overcome this lacuna, various surrogate models are integrated

with the process, which will make the complete process computationally efficient. Various works have been carried out considering different surrogate models. Utilizing the ANN model, Balokas et al. (2018), Kumar et al. (2017), Lefik et al. 2009), Malik and Arif (2013) analyzed the impact behavior of composites and FGM structures. Various researchers also consider different other surrogates like PNN, SVM, GPR, MARS during stochastic analysis. Dey et al. (2017) have compared various metamodels like MARS, ANN, PNN, MLS, SVR during stochastic dynamic analysis of laminated composites. Karsh et al. (2018) have used the MARS surrogate model for the natural frequency analysis of the FGM plate. In the present paper, the study considers MARS as a surrogate model for stochastic low-velocity impact analysis of FGM plate.

In the present study, the uncertain impact responses analysis of the FG plate (refer to Figure 1) is conducted for determining the outcome of impact angle, impactor's velocity, the mass density of impactor, and point of impact on the impact responses by employing the MARS model. The traditional MCS is conducted to capture the material properties' uncertainty. As already known, MCS requires a large number of simulations leading to higher computational cost ad time. Therefore, to minimize this drawback of MCS, the surrogate-based MARS model is used, reducing the number of simulations and ultimately lowering cost and time.

2 Theoretical Modeling

The equation for dynamic analysis is given by [Dey and Karmakar (2014)]

$$[M(\hat{\omega})]\{\ddot{\delta}\} + [K(\hat{\omega})]\{\delta\} = \{F\} \tag{1}$$

The contact force $\{F_C^*\}$ in the impact loading can be represented as

$$\{F\} = \{0\,0\,0\ \ldots F_C^* \ldots\ 0\,0\,0\}^T \tag{2}$$

The equation the impactor motion is given in Equation (3)

$$m_{(I)}\ddot{\delta}_{(I)} + F_C^* = 0 \tag{3}$$

Wherein $m_{(I)}$ and $\ddot{\delta}_{(I)}$ denotes impactor's mass and acceleration, respectively. The force when the elastic impactor touches the FGM plate is called the contact force and is determined by employing the modified Hertzian contact (MHC). Here, the impact loading is applied at the middle of the plate,

as shown in Figure 1. The contact force (F_C^*) for that is given by [Sun and Chen (1985)]

$$F_C^* = K_M \psi^{1.5} 0 < \psi \leq \psi_{\max} \tag{4}$$

$$K_M = \frac{16}{3\pi} \frac{1}{K_P + K_I} \sqrt{\frac{B}{\lambda}} \tag{5a}$$

Where K_M, ψ, and $\psi_{\max.}$ represent modified contact stiffness, local indentation, and maximum indentation, respectively [Larson (2006)]. λ is the constant, and for the present study, $\lambda = 2$ is considered. B is also a constant, which depends on the curvature of the impactor and target plate.

$$\frac{1}{B} = \frac{1}{R^{imp}} + \frac{1}{R^{plt}} \tag{5b}$$

where R^{imp} and R^{plt} is the radius of curvature of the impactor and plate, respectively. The local indentation can be obtained by

$$\psi(t) = \delta_I(t) Cos\theta - \delta_P(x_c, y_c, t) Cos\phi \tag{6}$$

Where δ_I is impactor deformation and δ_P is plate deformations, at point of loading (x_c, y_c) in the z-direction, while θ is oblique impact angle and ϕ is twist angle. At the loading point, the contact force components are

$$F_{ix} = 0, \quad F_{iy} = 0, \quad F_{iz} = F_C^* \tag{7}$$

The transient nature of the contact force (F_C^*) can be observed with Δt time intervals. Here, Newmark's integration scheme is employed for evaluating time-dependent equations. By applying the Newmark's integration scheme in Equations (1) and (3), succeeding equations at $(t + \Delta t)$ time can be obtained as

$$[\tilde{K}_P]\{\delta\}^{t+\Delta t} = \{\tilde{F}_C^*\}^{t+\Delta t} \tag{8}$$

$$[\tilde{K}_I]\{\delta_I\}^{t+\Delta t} = \{\tilde{F}_C^*\}^{t+\Delta t} \tag{9}$$

Where effective stiffness matrix for target plate is $[\tilde{K}_P]$ and for impactor is $[\tilde{K}_I]$ and is represented as

$$[\tilde{K}_P] = [K(\bar{\omega})] + [K_\sigma] + c_0[M(\bar{\omega})] \tag{10}$$

$$[\tilde{K}_I] = c_0 m_I \tag{11}$$

For $t+\Delta t$, the impact responses such as plate and impactor deformations are determined by

$$\{\bar{F}\}^{t+\Delta t} = \{F\} + \{F_C^*\}^{t+\Delta t} + [M(\bar{\omega})](c_0\{\delta_P\}^t + c_1\{\dot{\delta}_P\}^t + c_2\{\ddot{\delta}_P\}^t) \tag{12}$$

$$\delta_I = \frac{\bar{F}_I^{t+\Delta t}}{m_I} \tag{13}$$

where,

$$\bar{F}_I^{t+\Delta t} = m_I(c_0\delta_I^t + c_1\dot{\delta}_I^t + c_2\ddot{\delta}_I^t) - F_C^{*t} \tag{14}$$

Plate and impactor's acceleration and velocity can be calculated as

$$F_{ix} = 0, F_{iy} = 0, F_{iz} = F_C^* \tag{15}$$

$$\{\ddot{\delta}_P\}^{t+\Delta t} = c_0(\{\delta_P\}^{t+\Delta t} - \{\delta_P\}^t) - c_1\{\dot{\delta}_P\}^t - c_2\{\ddot{\delta}_P\}^t \tag{16}$$

$$\ddot{\delta}_I^{t+\Delta t} = c_0(\delta_I^{t+\Delta t} - \delta_I^t) - c_1\dot{\delta}_I^t - c_2\ddot{\delta}_I^t \tag{17}$$

$$\{\dot{\delta}_P\}^{t+\Delta t} = \{\dot{\delta}_P\}^t + c_3\{\ddot{\delta}_P\}^t + c_4\{\ddot{\delta}_P\}^{t+\Delta t} \tag{18}$$

$$\dot{\delta}_I^{t+\Delta t} = \dot{\delta}_I^{t\Delta t} + c_3\ddot{\delta}_I^t + c_4\ddot{\delta}_I^{t+\Delta t} \tag{19}$$

At initial boundary condition

$$\{\delta_P\} = \{\dot{\delta}_P\} = \{\ddot{\delta}_P\} = 0 \tag{20}$$

$$\delta_I = \ddot{\delta}_I = 0 \quad \text{and} \quad \dot{\delta}_I = V \tag{21}$$

where V is the initial velocity of the impactor. The value of constants of integration can be obtained by

$$c_0 = \frac{1}{X\Delta t^2}, \quad c_1 = \frac{1}{X\Delta t}, \quad c_2 = \frac{1}{2X} - 1,$$
$$c_3 = (1-Y)\Delta t, \quad c_4 = Y\Delta t \tag{22}$$

where $X = 0.5$ and $Y = 0.25$. Here, we have considered an isoparametric quadratic element for the FE formulation having eight nodes (refer to Figure 2). The expression for shape function $\hat{S}_i$ can be shown as

$$\hat{S}_i = \frac{(1+\vartheta\vartheta_i)(1+\varepsilon\varepsilon_i)(\varepsilon\varepsilon_i + \vartheta\vartheta_i - 1)}{4} \quad (\text{for } i = 1,2,3,4) \tag{23}$$

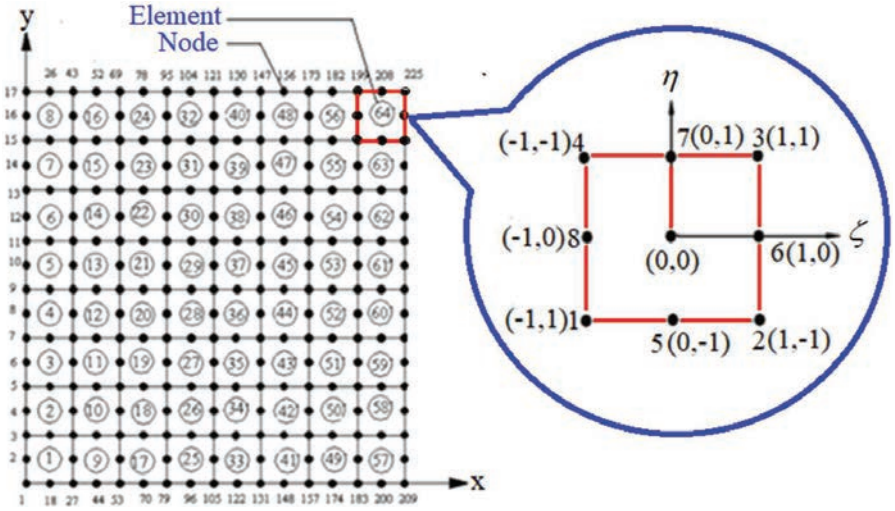

Figure 2 FE discretization of FG plate into 64 elements.

$$\hat{S}_i = \frac{(1-\vartheta^2)(1+\varepsilon\varepsilon_i)}{2} \quad (\text{for } i = 5, 7) \tag{24}$$

$$\hat{S}_i = \frac{(1-\varepsilon^2)(1+\vartheta\vartheta_i)}{2} \quad (\text{for } i = 6, 8) \tag{25}$$

Where for element, the local natural coordinates are represented by ε and ϑ. In the case of FGM, the material properties gradation takes place following different laws. Here, we have considered power law, which is given as [21]

$$E(\hat{\omega}) = E_{Al} + (E_{Zr} - E_{Al})\left[\frac{z}{t} + \frac{1}{2}\right]^p \tag{26}$$

$$\mu(\hat{\omega}) = \mu_{Al} + (\mu_{Zr} - \mu_{Al})\left[\frac{z}{t} + \frac{1}{2}\right]^p \tag{27}$$

$$\rho(\hat{\omega}) = \rho_{Al} + (\rho_{Zr} - \rho_{Al})\left[\frac{z}{t} + \frac{1}{2}\right]^p \tag{28}$$

Where E_{Al}, E_{Zr}, μ_{Al}, μ_{Zr}, and ρ_{Al}, ρ_{Zr} are the elastic modulus, Poisson's ratio, and mass density of aluminium and zirconia, respectively. 'p' shows the power-law index and 'h' is the plate thickness, while $(\hat{\omega})$ represents the degree of stochasticity.

3 Multivariate Adaptive Regression Splines (MARS)

MARS is the nonparametric regression statistical approach that is iterative, like a machine learning model [Friedman (1999)]. There is no relationship between response and predictor variable. In the MARS model, training data sets are first divided into splines (linear segments) with different slops called basic functions. Each collection of training data have a separate regression model. The regression lines are connected by using the knots. The MARS model searches for the best location for the knots having the pair of basic functions [Zhang and Goh (2016)]. The basic functions are increased continuously until the number of basic functions reached the maximum level. The MARS algorithm's second step removes the insignificant redundant basic function [Dey et al. (2016)]. The MARS model $f(x)$ with basic function and interaction can be written as

$$f(x) = \gamma_0 + \sum_{n=1}^{M} \gamma_n \beta_n^f(z_i) \tag{29}$$

where γ is the constant-coefficient and β_n is the basic function which can be shown as

$$\beta_n^f(z_i) = \prod_{i=1}^{i_n} [Y_{i,n}(z_{j(i,n)} - q_{i,n})]_T^g \tag{30}$$

where i_n denotes the interaction order $Y_{i,n} = \pm 1$, $z_{j(i,n)}$ represents the jth variable, $1 \leq j(i,n) \leq m$, and $q_{i,n}$ is the knot position of corresponding variables. 'T' means a truncated power function. The basic function may be in the following shapes

$$[Y_{i,n}(z_{j(i,n)} - q_{i,n})]_T^g = [Y_{i,n}(z_{j(i,n)} - q_{i,n})]^g \quad \text{for } [Y_{i,n}(z_{j(i,n)} - q_{i,n})] < 0 \tag{31}$$

$$[Y_{i,n}(z_{j(i,n)} - q_{i,n})] = 0, \quad \text{Otherwise} \tag{32}$$

Thus, all basic function can be written as

$$A = \{[Y_{i,n}(z_{j(i,n)} - q_{i,n})]_T^g\}, \quad q \in \{z_{1j}, z_{2j}, \ldots\ldots z_{Mj}\} \tag{33}$$

Here, uncertainty in all four material properties is considered. The value for which is considered as $\pm 10\%$. The complete methodology for the present work is represented in Figure 3. The outcomes of the oblique impact angle,

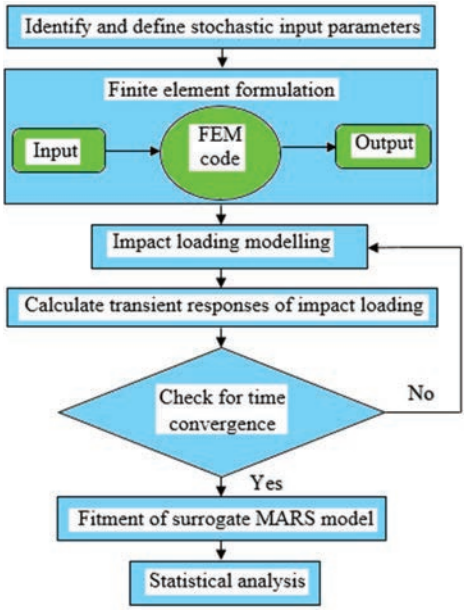

Figure 3 Flowchart representing the present study complete methodology.

the impactor's velocity, the impactor's mass density, and the point of impact on the impact responses are determined.

The stochastic input variables are following:

1. Compound effect of source uncertainties

$$\psi\{E(\omega), G(\omega), \mu(\omega), \rho(\omega)\} = \Phi[\{E(z)\}(\omega), \{G(z)\}(\omega), \{\mu(z)\}(\omega), \{\rho(z)\}(\omega)]$$

2. For impact angle (ϕ)

$$\Psi(\phi) = \Phi[\phi, \{E(z)\}(\omega), \{G(z)\}(\omega), \{\rho(z)\}(\omega), \{\mu(z)\}(\omega)]$$

3. For the velocity of the impactor (V)

$$\Psi(V) = \Phi[V, \{E(z)\}(\omega), \{G(z)\}(\omega), \{\rho(z)\}(\omega), \{\mu(z)\}(\omega)]$$

4. For the mass density of the impactor

$$\Psi(\rho) = \Phi[\rho, \{E(z)\}(\omega), \{G(z)\}(\omega), \{\rho(z)\}(\omega), \{\mu(z)\}(\omega)]$$

5. For the point of impact loading

$$\Psi(l) = \Phi[l, \{E(z)\}(\omega), \{G(z)\}(\omega), \{\rho(z)\}(\omega), \{\mu(z)\}(\omega)]$$

Where, Φ is the MCS operator, while l is the point of impact loading. In the past, some works on the stochastic analysis of layered structures by using the MCS were performed [Karsh et al. (2018a), (2018b), Mukhopadhyay et al. (2018), Kumar et al. (2019)] using different surrogate models such as ANN, PNN. It was found by using the surrogate; we can significantly reduce the sample size without compromising the accuracy of the results.

4 Results and Discussion

The various material properties considered are as $E_{Al} = 70$ Gpa, $E_{Zr} = 151$ Gpa, $\upsilon_{Al} = 0.25$, $\upsilon_{Zr} = 0.30$, $\rho_{Al} = 2707$ Kg/m^3, $\rho_{Zr} = 3000$ Kg/m^3 [Karsh et al. (2018)]. The material properties gradation is done utilizing the power-law considering the power-law index as 1. The dimensions of the FGM plate are considered as $L = b = 1$ m, $h = 0.002$ m subjected to impact loading at point 2 (refer Figure 8(d)). If otherwise mentioned, consider $p = 1$, $V = 5$ m/sec, $\phi = 0^\circ$, T = 300 K, $h = 0.002$ m, $\rho_{imp} = 85 \times 10^{-4} N - s^2/cm^4$. For the FE formulation, the discretization is done considering (8×8) mesh size having 64 elements having eight nodes, wherein each node having five degree of freedom (dof), as shown in Figure 2. The present study's validation is carried out by comparing results with those already present in literature [Kiani et al. (2013)], as shown in Figure 4. The validation graph shows that the present result is approximately similar to that of the past results. The tabulated values of validation are presented in Table 1. This paper performs the low-velocity impact analysis of the FGM cantilever plate using the deterministic and stochastic approaches. The results of the deterministic approach are shown in Figures 5 to 8. Figure 5 illustrates the outcome of impact angle in which contact force and plate deformation decrease with an increase in the impact angle. In contrast,

Table 1 Validation of present results with previously published results [Kiani et al. (2013)] considering the boundary condition as mentioned in Figure 4(i)

Contact Force (N)	Kiani et al. (2013)	Present Study	% Error
Min value	0	0	0
Max value	1019	1037	1.766
Mean value	517.1	523.8	1.295
Standard Deviation	330.2	320.6	−2.907

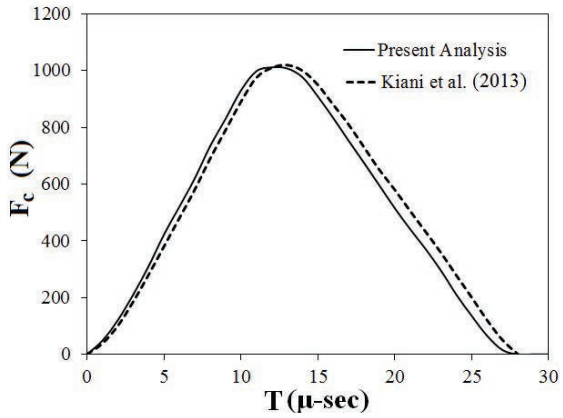

Figure 4(i) Validation of present results with previous published results [Kiani et al. (2013)], Time history of contact force for Silicon Nitride and Stainless Steel FGM beam clammed at both end considering time step $\Delta T = 1.0$ μ-sec. length (L) = 135 mm, width (b) = 15 mm, thickness (h) = 10 mm, impactor mass = 0.01 Kg, radius of impactor = 12.7 mm, and initial velocity of impactor = 1.0 m/s.

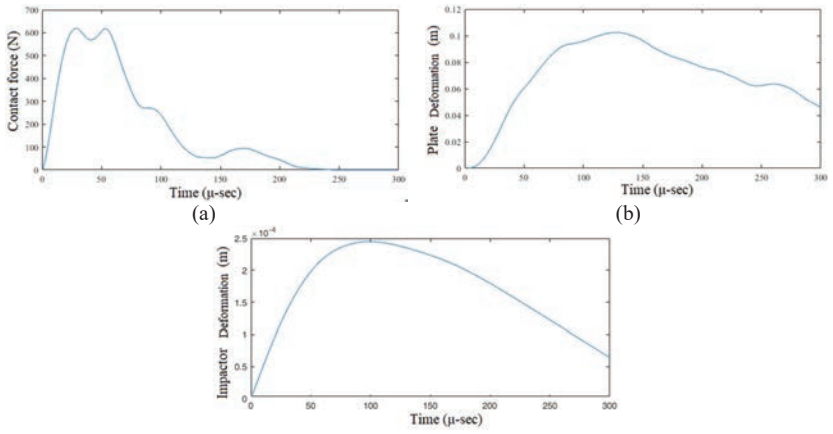

Figure 4(ii) Time histories of impact responses at centre of FGM cantilever plate with considering L = b = 1 m, h = 0.002 m, p = 1, V = 5 m/sec, $\phi = 0^\circ$, T = 300K, h = 0.002 m, $\rho_{imp} = 85 \times 10^{-4} N - s^2/cm^4$.

impactor deformation increases with an increase in the impact angle from 0° to 45°.

The outcome of the impactor's velocity is shown in Figure 6. It was found that all impact responses are increased with an increase in the impactor's

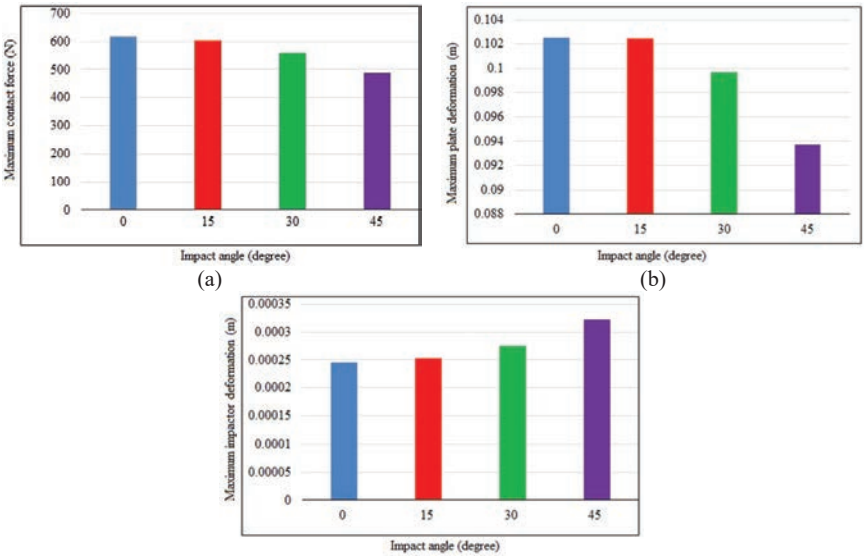

Figure 5 Influence of impact angle on transient impact responses considering consider p = 1, V = 5 m/sec, T = 300K, h = 0.002 m, $\rho_{imp} = 85 \times 10^{-4} N - s^2/cm^4$ at location 2 (Figure 8(d)).

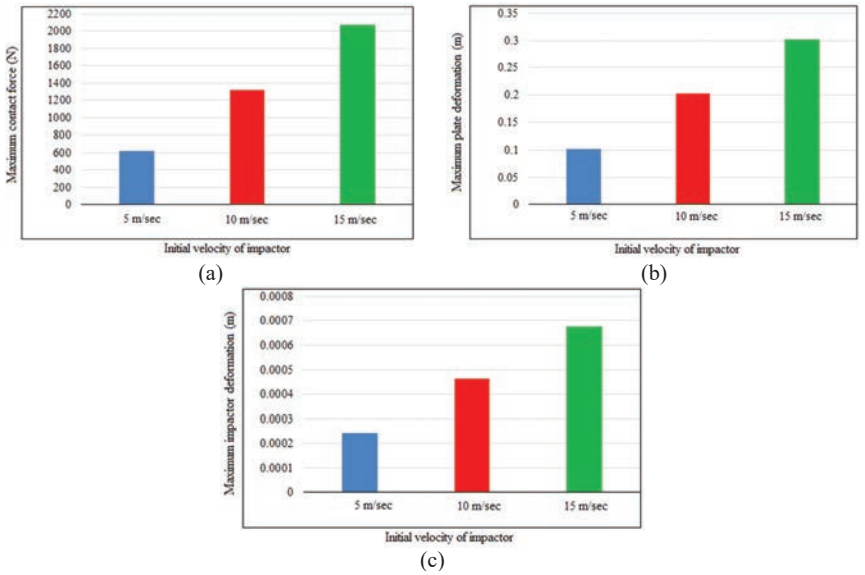

Figure 6 Influence of velocity of impactor on transient impact responses considering p = 1, $\phi = 0^\circ$, T = 300K, h = 0.002 m, $\rho_{imp} = 85 \times 10^{-4} N - s^2/cm^4$ at location 2 (Figure 8(d)).

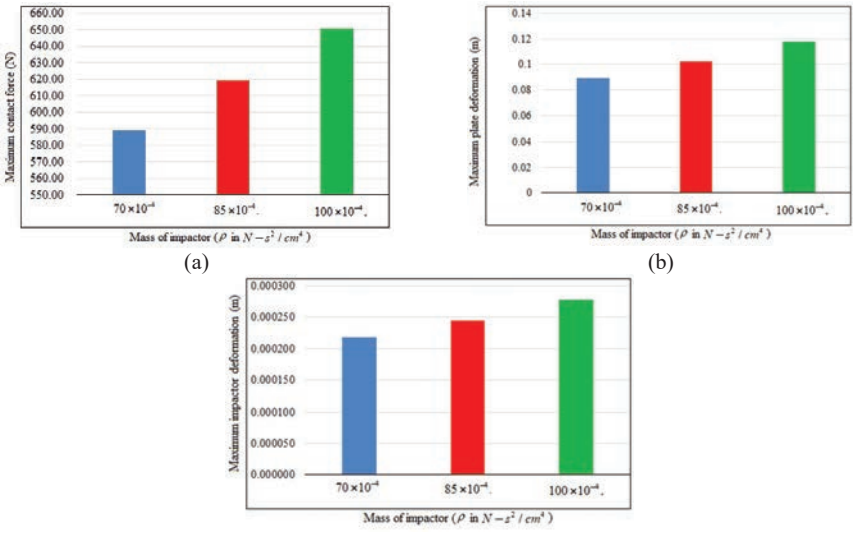

Figure 7 Influence of mass of impactor on transient impact responses considering p = 1, V = 5 m/sec, $\phi = 0°$, T = 300K, h = 0.002 m.

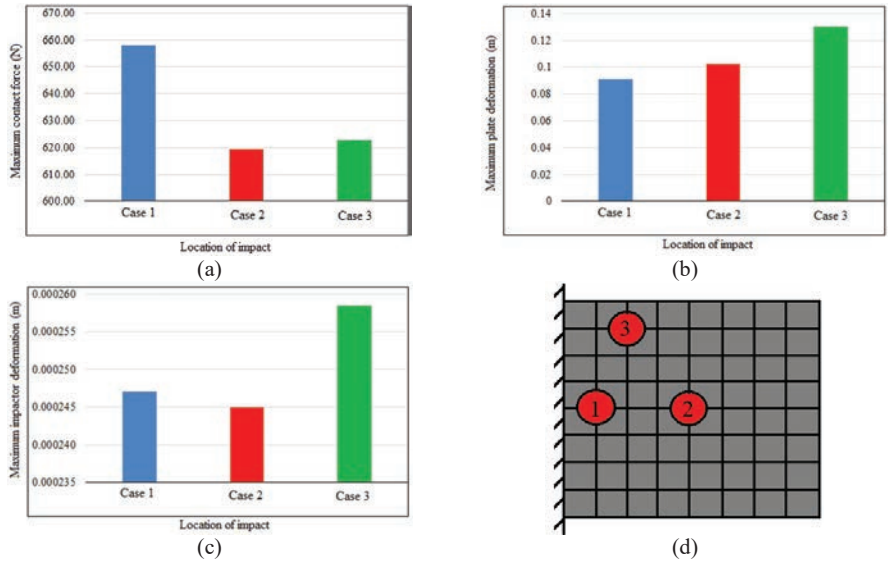

Figure 8 Influence of point of impact (refer figure 8(d)) on transient impact responses considering p = 1, V = 5 m/sec, $\phi = 0°$, T = 300K, h = 0.002 m, $\rho_{imp} = 85 \times 10^{-4} N - s^2/cm^4$.

Table 2 Convergence study of the sample size of MARS model

Impact Responses	Method	Sample Size	Maximum	Minimum	Mean	Standard Deviation
Peak	MCS	2100	620.4906	598.8708	611.4041	3.2759
Contact	MARS	128	624.1848	597.0768	611.2439	4.1419
force (N)		256	625.6470	599.5029	612.4050	3.8861
		512	621.7845	601.2292	611.8448	3.2606
Peak	MCS	2100	0.1072	0.1012	0.1044	860.72×10^{-6}
Plate	MARS	128	0.1082	0.1008	0.1044	0.0011
deformation		256	0.1077	0.1014	0.1043	934.34×10^{-6}
(m)		512	0.1073	0.1017	0.1044	861.76×10^{-6}
Peak	MCS	2100	0.0002522	0.0002428	0.0002481	1.3015×10^{-6}
Impactor	MARS	128	0.0002542	0.0002421	0.0002481	1.8186×10^{-6}
deformation		256	0.0002566	0.0002406	0.0002480	1.8257×10^{-6}
(m)		512	0.0002522	0.0002438	0.0002810	1.3920×10^{-6}

Table 3 Parametric study on the effect of different parameters on impact responses

Parameters		Max. Contact Force (N)	Max. Plate Deformation (m)	Max. Impactor Deformation (m)
Impact	0°	619.38	0.102521	0.000245
angle	15°	602.20	0.102413	0.000253
	30°	559.35	0.0997	0.000275
	45°	486.83	0.093742	0.000322
Impact	5	619.38	0.102521	0.000245
velocity	10	1323.49	0.202239	0.000464
(m/s)	15	2069.40	0.301318	0.000677
Mass of	70×10^{-4}	589.10	0.089252	0.000218
impactor	85×10^{-4}	619.38	0.102521	0.000245
$(N - s^2/cm^4)$	100×10^{-4}	650.94	0.117787	0.000277
Location of	Case 1	658.05	0.091265	0.000247
Impact	Case 2	619.38	0.102521	0.000245
	Case 3	622.72	0.130276	0.000258

velocity due to the rise in the impactor's kinetic energy. Figure 7 presents the outcome of the impactor's mass density on the impact responses and found that all impact responses increase with an increase in the impactor's mass density. Figure 8 shows the outcome of the point of impact loading (refer to Figure 8(d)) it was found that contact force is maximum at point 1, while the minimum for point 2.

In the stochastic approach, Monte Carlo simulation along with the MARS model is employed. The MCS required thousands of iterations which makes the process exhaustive. So, to overcome this disadvantage of MCS, a surrogate-based MARS model is applied to reduce the number of simulations with reasonable accuracy. The MARS model is used to determine the impact responses such as maximum contact force, impactor, and plate deformation. First, a convergence study of the MARS model's sample size is carried out as shown in Table 2, in which, with increasing the sample size, results of the MARS model are closer to the MCS. From the convergence study, it is confirmed that sample size 512 gives better results with significant accuracy. Further, to verify this statement, we have plotted the scatter plots shown in Figure 9. Considering the sample size 512, from the plot, there is a minimum deviation between the results of surrogate and MCS. In addition to it, PDF plots also presented showcasing the MARS results (for different sample sizes) and are compared with MCS results for all impact responses, as shown in Figure 10. For the sample size 512, the plot is nearer to the MCS. This indicates that the MARS model is well fitted with MCS. After achieving the required sample size, a further probabilistic investigation is carried out. Figure 11 illustrates the influence of the different degrees of stochasticity (C $\pm$ 5%, 10%, 20%) in all the material properties of FGM on the transient impact responses. It was found that on incrementing the degree of stochasticity, the area of bound increases. The outcome of impact angle is shown in Figure 12, wherein contact force and plate deformation decreased with an increase in impact angle from 0° to 45°, while impactor deformation increase with the rise in impact angle.

Figure 13 illustrates probability density function plots to show the impactor's velocity (V) effect. All the responses significantly increase with the impactor's velocity due to increased impactor's kinetic energy. The probability density function plots showing the effects of mass density are illustrated in Figure 14, wherein all impact responses increase with an increase in the impactor's mass density. The effects of point of impact loading are shown in Figure 15, wherein contact force is minimum at point 2.

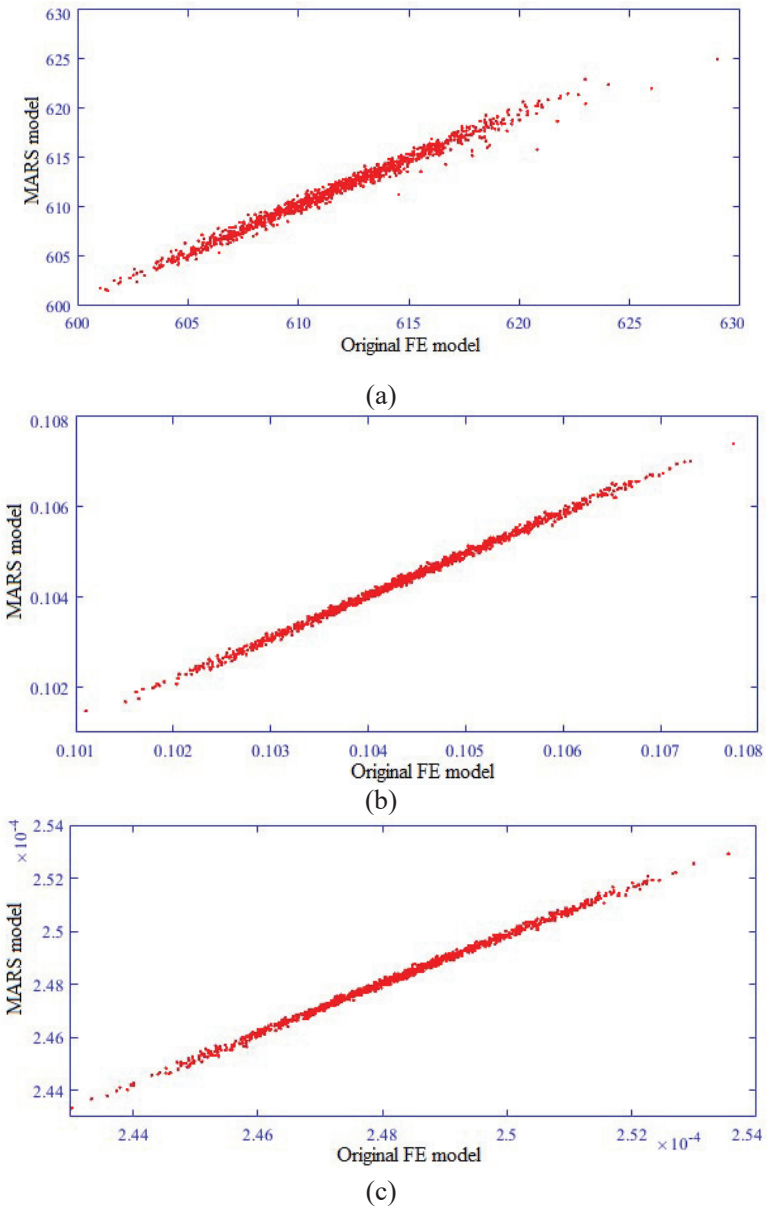

Figure 9 Scatter plots between original FE model and MARS model for impact responses (max. contact force, max. plate deformation, and max. impactor deformation) with considering sample size (N) = 512.

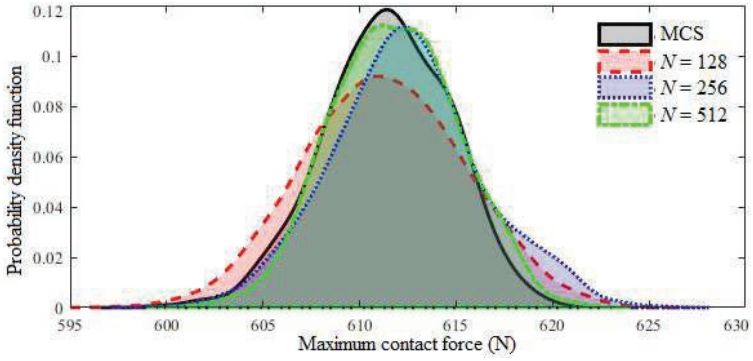

(a)

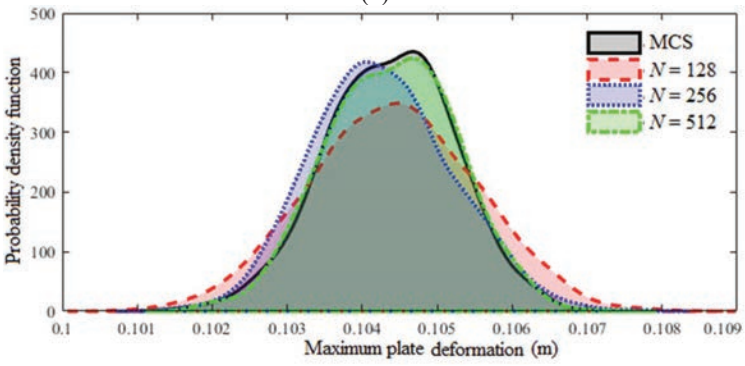

(b)

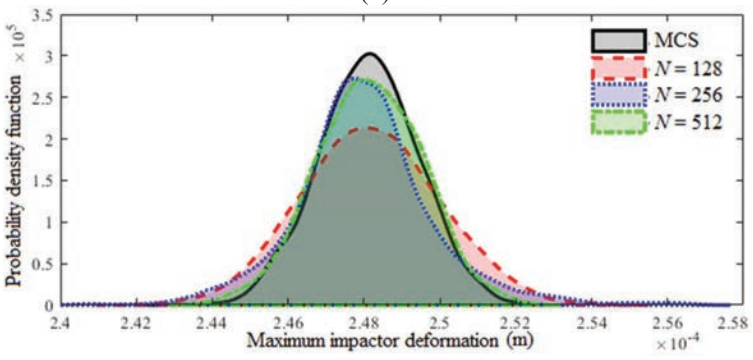

(c)

Figure 10 PDF plots between original FE model and MARS model for impact responses (max. contact force, max. plate deformation, and max. impactor deformation) with different sample size (N).

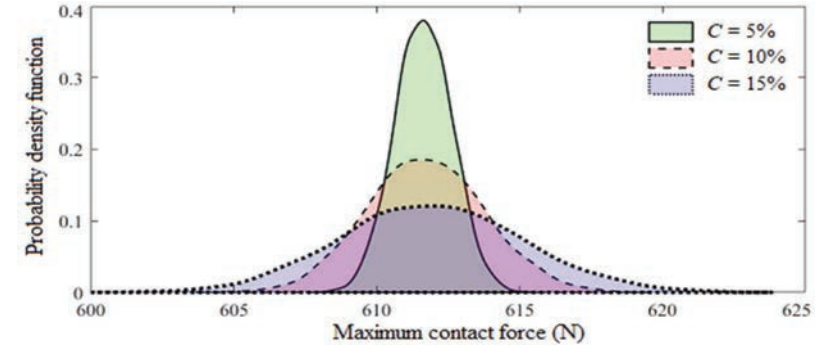

(a)

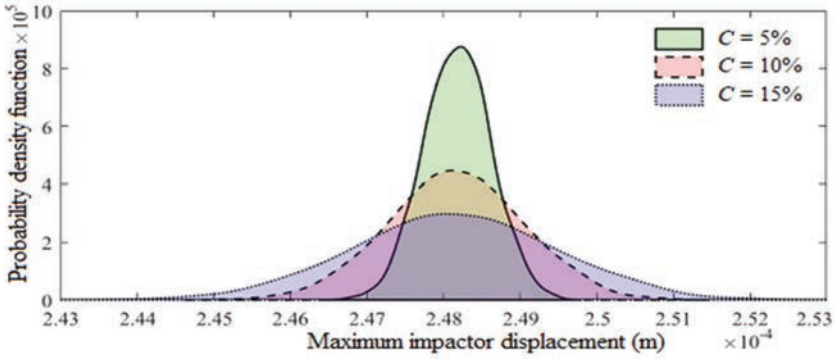

(b)

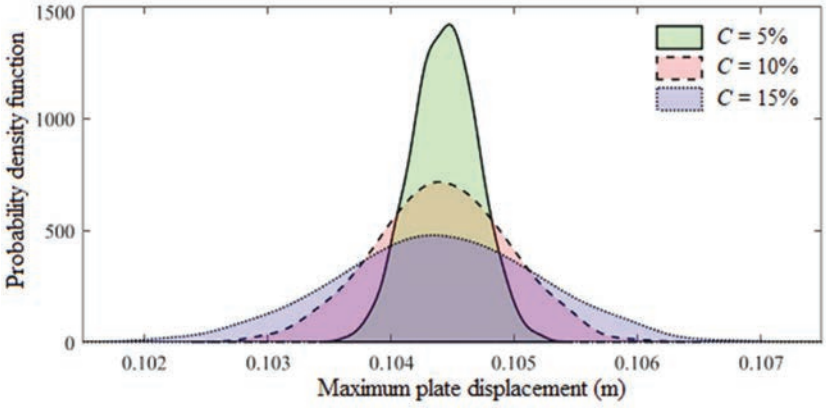

(c)

Figure 11 Influence of the degree of stochasticity (C) considering compound effect of source uncertainties.

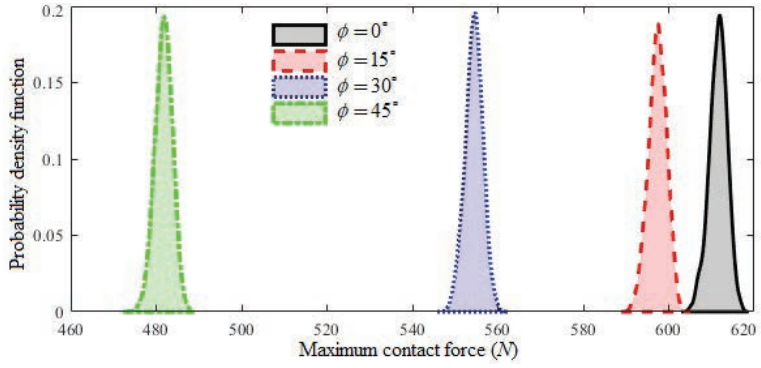

(a)

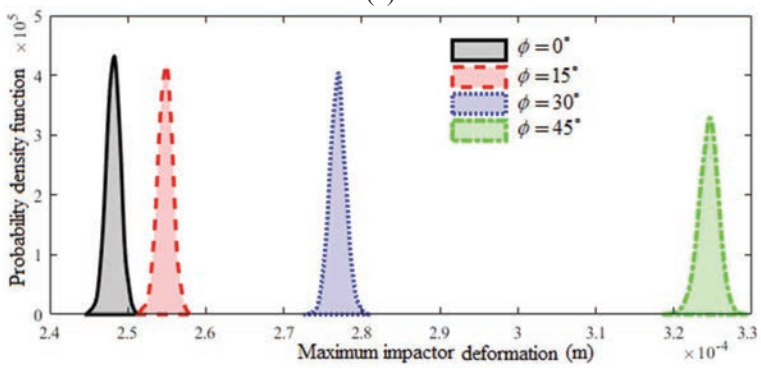

(b)

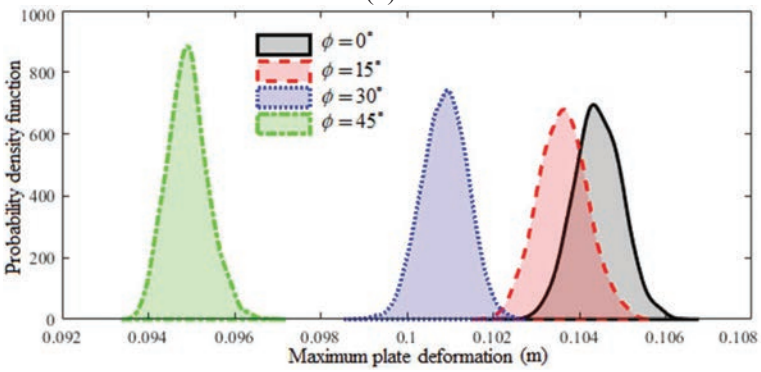

(c)

Figure 12 Influence of impact angle on stochastic transient impact responses considering consider $p = 1$, $V = 5$ m/sec, T = 300K, $h = 0.002$ m, $\rho_{imp} = 85 \times 10^{-4} N - s^2/cm^4$ at location 2 (Figure 8(d)).

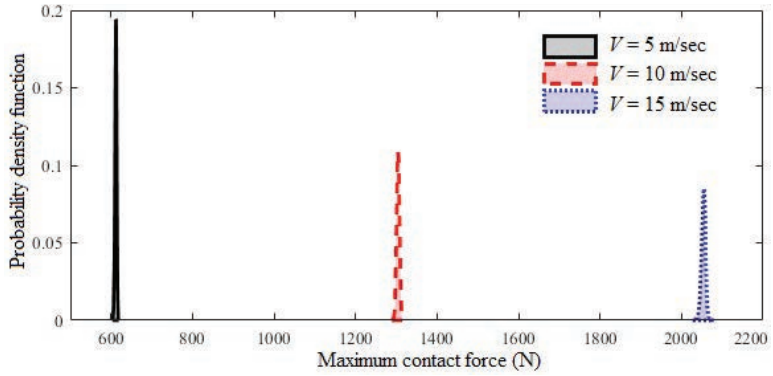

(a)

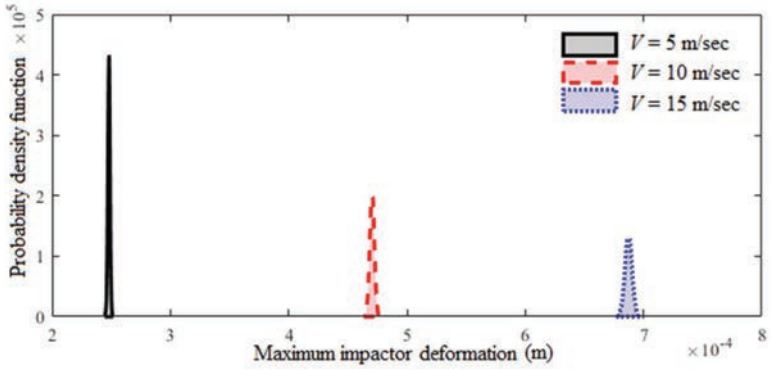

(b)

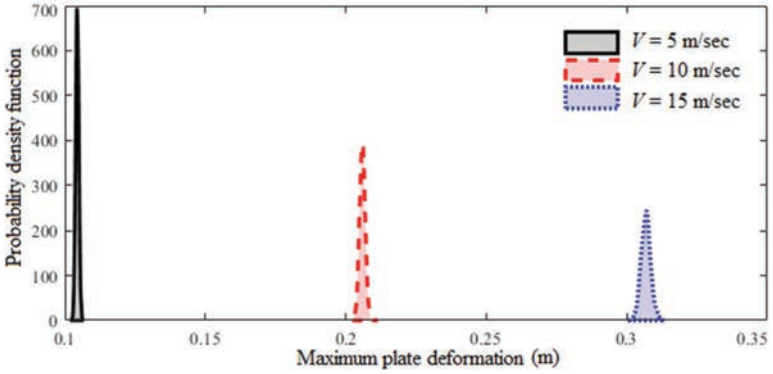

(c)

Figure 13 Influence of velocity of impactor (V) on stochastic transient impact responses considering $p = 1$, $\phi = 0°$, T = 300K, $h = 0.002$ m, $\rho_{imp} = 85 \times 10^{-4} N - s^2/cm^4$ at location 2 (Figure 8(d)).

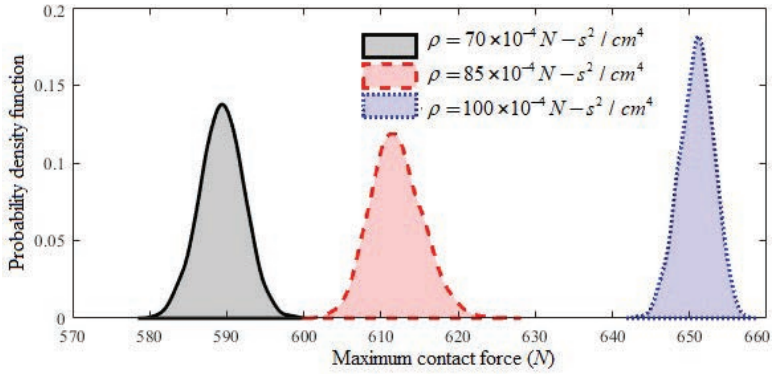

(a)

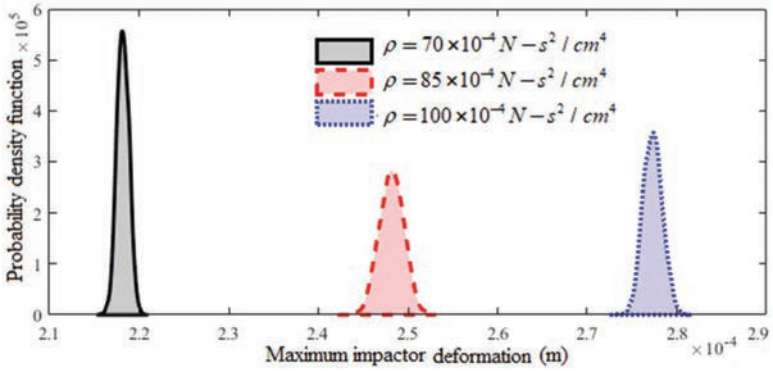

(b)

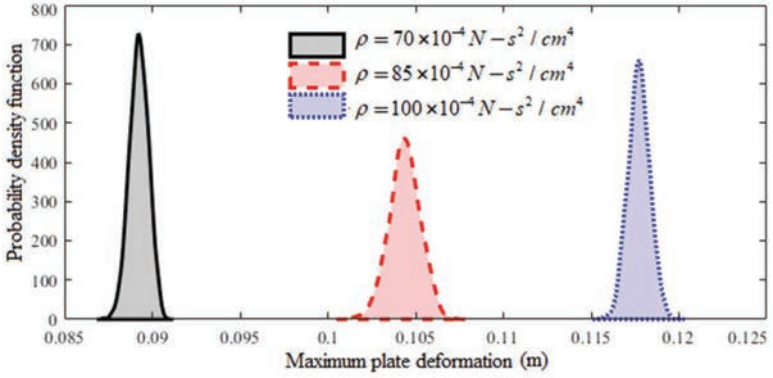

(c)

Figure 14 Influence of mass of impactor (ρ) on stochastic transient impact responses considering $p = 1$, $V = 5$ m/sec, $\phi = 0°$, T = 300K, $h = 0.002$ m.

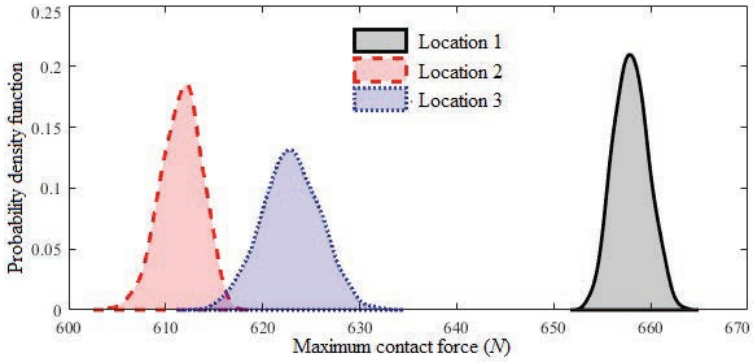

(a)

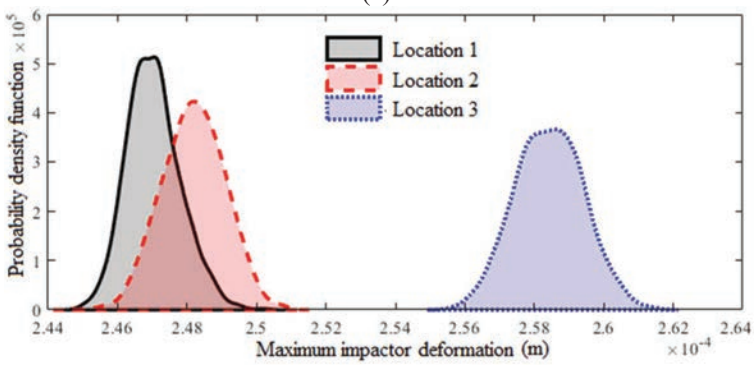

(b)

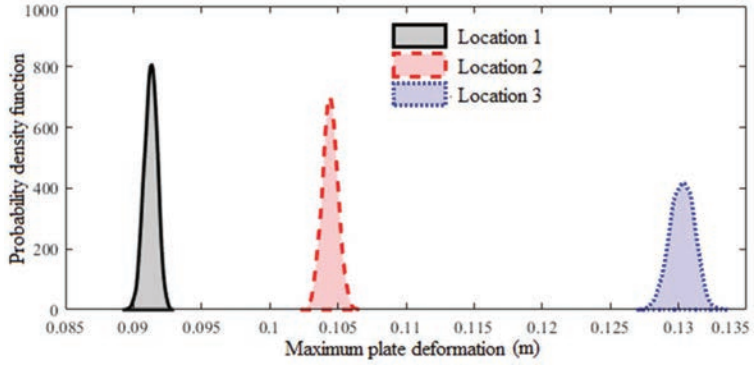

(c)

Figure 15 Influence of point of impact (refer Figure 8(d)) on stochastic transient impact responses considering $p = 1$, $V = 5$ m/sec, $\phi = 0^\circ$, T = 300K, $h = 0.002$ m, $\rho_{imp} = 85 \times 10^{-4} N - s^2/cm^4$.

5 Conclusions

The novelty of the present study includes the deterministic and stochastic low-velocity impact responses analysis of the FGM cantilever plate by employing the surrogate-based MARS model. The combined effects of stochasticity in the FGM plate's material properties are considered random input parameters. The modified contact law and NTI approaches are utilized to determine the stochastic transient impact responses. The FE code is developed for the present analysis. MARS model is integrated with the MCS for constructing an efficient computational framework. The convergence study is carried out to obtain the optimum sample size of the MARS model. The parametric study finds the response of various input parameters on the stochastic transient low-velocity impact responses. The results illustrate that all the parameters such as impact angle, the mass density of impactor, and initial velocity of impactor significantly affect the impact responses. In the future, the employed framework can be utilized for the other dynamic analysis of layered structures.

References

Apetre, N. A., Sankar, B. V., and Ambur, D. R., (2006), "Low-velocity impact response of sandwich beams with functionally graded core, International Journal of Solids and Structures, Vol. 43 No. 9, pp. 2479–2496.

Atmane, H. A., Tounsi, A., Ziane, N., and Mechab, I. (2011), "Mathematical solution for free vibration of sigmoid functionally graded beams with varying cross-section", Steel and Composite Structures, 11(6), 489–504.

Bathe, KJ, (1990), Finite Element Procedures in Engineering Analysis. PHI, New Delhi, India.

Belkorissat, I., Houari, M. S. A., Tounsi, A., Bedia, E. A., and Mahmoud, S. R. (2015). "On vibration properties of functionally graded nano-plate using a new nonlocal refined four variable model". Steel Compos. Struct, 18(4), 1063–1081.

Chaht, F. L., Kaci, A., Houari, M. S. A., Tounsi, A., Bég, O. A., and Mahmoud, S. R. (2015). "Bending and buckling analyses of functionally graded material (FGM) size-dependent nanoscale beams including the thickness stretching effect". Steel and Composite Structures, 18(2), 425–442.

Chelu, P. and Librescu, L., (2006), "Low-velocity impact on a functionally graded circular thin plate", In ASME 8th Biennial Conference on

Engineering Systems Design and Analysis, American Society of Mechanical Engineers, pp. 791–800.

Darilmaz, K. (2015), "Vibration analysis of functionally graded material (FGM) grid systems", Steel and Composite Structures, 18(2), 395–408.

Dey S., Karmakar A. (2014), "Effect of oblique angle on low velocity impact response of delaminated composite conical shells", Journal of Mechanical Engineering Science Proc IMechE Part C, Vol. 228(15), pp. 2663–2677.

Dey, S. and Karmakar, A., (2014a), "Effect of oblique angle on low velocity impact response of delaminated composite conical shells", Proceedings of the Institution of Mechanical Engineers, Part C: Journal of Mechanical Engineering Science, Vol. 228, No. 15, pp. 2663–2677.

Dey, S. and Karmakar, A., (2014b), "Time dependent response of low velocity impact induced composite conical shells under multiple delamination", Mechanics of Time-Dependent Materials, Vol. 18 No. 1, pp. 55–79.

Dey, S., Adhikari, S. and Karmakar, A., (2015), "Impact response of functionally graded conical shells", Latin American Journal of Solids and Structures, Vol. 12 No. 1, pp. 133–152.

Dey, S., Mukhopadhyay, T., Naskar, S., Dey, T. K., Chalak, H. D. and Adhikari, S., (2016) "Probabilistic characterisation for dynamics and stability of laminated soft core sandwich plates", Journal of Sandwich Structures & Materials, p. 1099636217694229.

Etemadi, E., Khatibi, A.A. and Takaffoli, M., (2009), "3D finite element simulation of sandwich panels with a functionally graded core subjected to low velocity impact", Composite Structures, Vol. 89 No. 1, pp. 28–34.

Fekrar, A., El Meiche, N., Bessaim, A., Tounsi, A., and Adda Bedia, E. A. (2012). "Buckling analysis of functionally graded hybrid composite plates using a new four variable refined plate theory". Steel and Composite Structures, 13(1), 91–107.

Friedman, J. H., (1991), "Multivariate adaptive regression splines", The annals of statistics, Vol. 19, No. 1, pp. 1–67.

Fu, Y., Hu, S. and Mao, Y., (2016), "Nonlinear low-velocity impact analysis of functionally graded shallow spherical shells in thermal environments", Journal of Thermoplastic Composite Materials, Vol. 29, No. 5, pp. 680–703.

Gong, S. W., Lam, K. A. and Reddy, J.N., (1999), "The elastic response of functionally graded cylindrical shells to low-velocity impact", International Journal of Impact Engineering, Vol. 22 No. 4, pp. 397–417.

He, W., Yao, L., Meng, X., Sun, G., Xie, D. and Liu, J., (2019), "Effect of structural parameters on low-velocity impact behavior of aluminum honeycomb sandwich structures with CFRP face sheets", Thin-Walled Structures, Vol. 137, pp. 411–432.

Hou, Y., Tie, Y., Li, C., Sapanathan, T. and Rachik, M., (2019), "Low-velocity impact behaviors of repaired CFRP laminates: Effect of impact location and external patch configurations", Composites Part B: Engineering, Vol. 163, pp. 669–680.

Karsh, P. K., Mukhopadhyay, T., Dey, S., (2018c), "Stochastic dynamic analysis of twisted functionally graded plates", Composites Part B: Engineering, Vol. 147, pp. 259–278.

Karsh, P. K., Mukhopadhyay, T. and Dey, S., (2018a), "Spatial vulnerability analysis for the first ply failure strength of composite laminates including effect of delamination", Composite Structures, Vol. 184, pp. 554–567.

Karsh, P. K., Mukhopadhyay, T. and Dey, S., (2018b), "Stochastic Investigation of Natural Frequency for Functionally Graded Plates", In IOP Conference Series: Materials Science and Engineering, Vol. 326, No. 1, p. 012003.

Karsh, P. K., Mukhopadhyay, T. and Dey, S., (2019), "Stochastic low-velocity impact on functionally graded plates: Probabilistic and non-probabilistic uncertainty quantification", Composites Part B: Engineering, Vol. 159, pp. 461–480.

Kiani Y., Sadighi M., Salami S. J, and Eslami MR, (2013), "Low velocity impact response of thick FGM beams with general boundary conditions in thermal field", Composite Structures, Vol. 104, pp. 293–303.

Kumar, R. R., Mukhopadhyay, T., Pandey, K. M. and Dey, S., (2019), "Stochastic buckling analysis of sandwich plates: The importance of higher-order modes", International Journal of Mechanical Sciences, Vol. 152, pp. 630–643.

Larson, Reid A., Palazotto A. (2006), Low velocity impact analysis of functionally graded circular plates. In ASME 2006 International Mechanical Engineering Congress and Exposition, American Society of Mechanical Engineers, pp. 571–580.

Loy, C. T., Lam, K. Y., Reddy, J. N. (1999), Vibration of functionally graded cylindrical shells, International Journal of Mechanical Sciences, vol. 41, pp. 309–324.

Mars, J., Chebbi, E., Wali, M. and Dammak, F., (2018), "Numerical and experimental investigations of low velocity impact on glass fiber-reinforced polyamide", Composites Part B: Engineering, Vol. 146, pp. 116–123.

Mukhopadhyay, T., Naskar, S., Karsh, P. K., Dey, S. and You, Z., (2018), "Effect of delamination on the stochastic natural frequencies of composite laminates", Composites Part B: Engineering, Vol. 154, pp. 242–256.

Shariyat, M., Nasab, F. F., (2014), Low-velocity impact analysis of the hierarchical viscoelastic FGM plates, using an explicit shear-bending decomposition theory and the new DQ method. Composite Structures, Vol. 113, pp. 63–73.

Shariyat, M., and Jafari, R., (2013a), "Nonlinear low-velocity impact response analysis of a radially preloaded two-directional-functionally graded circular plate: A refined contact stiffness approach", Composites Part B: Engineering, Vol. 45, No. 1, pp. 981–994.

Shariyat, M., and Jafari, R., (2013b), "A micromechanical approach for semi-analytical low-velocity impact analysis of a bidirectional functionally graded circular plate resting on an elastic foundation", Meccanica, Vol. 48, No. 9, pp. 2127–2148.

Singh, H., Hazarika, B. C., and Dey, S., (2017), "Low velocity impact responses of functionally graded plates", Procedia engineering, Vol. 173, pp. 264–270.

Sun, C. T., Chen, J. K., (1985), On the impact of initially stressed composite laminates. Composite Materials, Vol. 19, pp. 490–504.

Tebboune, W., Benrahou, K. H., Houari, M. S. A., and Tounsi, A. (2015). "Thermal buckling analysis of FG plates resting on elastic foundation based on an efficient and simple trigonometric shear displacement theory". Steel and Composite Structures, 18(2), 443–465.

Zhang, W., and Goh, A. T., (2016), "Multivariate adaptive regression splines and neural network models for prediction of pile drivability", Geoscience Frontiers, Vol. 7 No. 1, pp. 45–52.

Biographies

P. K. Karsh received the bachelor's degree in Industrial and Produnction Engineering from Guru Ghasdas Central University, Bilaspur, India in 2012, the master's degree in Industrial and Produnction Engineering from Natioal Institute of Technology, Kurukshetra, India in 2016, and the philosophy of doctorate degree in Mehcnaical Engineering from Natioal Institute of Technology Silchar, India in 2019, respectively. He is currently working as an Assistant Professor at the Department of Mechanical Engineering, Faculty of Engineering & Technology, Parul University, India. His research areas include, stochastic free vibration analysis, impact analysis and failure analysis of composite and functionally graded materials. He has been serving as a reviewer for many highly-respected journals.

Bindi Thakkar received the bachelor's degree in Industrial and Mechanical Engineering from D. Y. Patil College of Engineering Pune, India in 2006, the master's degree in CAD/CAM from Bharti Vidhyapeeth University, Pine India in 2009, and pursuing PhD in Design and Manufacturing from Parul University in 2020 respectively. She is currently working as Head of

the Department and Assistant Professor at the Department of Mechanical Engineering, Faculty of Engineering & Technology, Diploma Studies, Parul University, India. She has 14 years of teaching experience at Parul University, since 2008. Her research areas include, Composites, stochastic free vibration analysis, impact analysis and failure analysis of composite and functionally graded materials.

R. R. Kumar received the bachelor's degree in Mechanical Engineering from Rajasthan Technical University, Kota, India in 2014, the master degree in Mechanical Engineering from National Institute of Technology, Silchar, India in 2016, and the doctor of Philosophy degree in Mechanical Engineering from National Institute of Technology Silchar, India in 2019, respectively. His research area includes: composite structure, stochastic analysis, surrogate modelling, impact analysis, vibration analysis and computational mechanics. He has been serving as a reviewer for several international journals.

Vaishali received the bachelor's degree in Mechanical Engineering from Noida Institute of Engineering and Technology, Greater Noida, India in

2014, the master's degree in Materials and Manufacturing Technology from National Institute of Technology, Silchar, India in 2018. She is currently pursuing her philosophy of doctorate degree in Mehcnaical Engineering from National Institute of Technology Silchar, India. Her research areas include, stochastic free vibration analysis, impact analysis, functionally graded materials, sandwich structures and hybrid structures.

Sudip Dey is a faculty in the Mechanical Engineering Department of National Institute of Technology Silchar, India. Previously, He was a Post-doctoral Researcher at Leibniz-Institut für Polymerforschung Dresden e. V., Germany. Prior to that he was a Post-doctoral Researcher at College of Engineering, Swansea University, United Kingdom. He obtained Bachelor in Mechanical Engineering Degree from Jadavpur University, India. He received Ph.D. (Engg.) degree from Jadavpur University, India. His field of specialization is Applied Mechanics and Design. He has more than fifteen years of experience in research, teaching, industrial and professional activities. He is actively engaged in academics, teaching, research and industrial projects. His research interests include molecular dynamics, multi-scale and computational investigation of fibre-matrix interaction, uncertainty quantification, mechanics of composite and functionally graded structures, finite element analyses, digital twin with an emphasis on computational modelling.